11^{th} International Conference on Fracture Mechanics of Concrete and Concrete Structures
FraMCoS-11
J. M. Chandra Kishen, A. Ramaswamy, S. Ray and R. Vidyasagar (Eds)
https://doi.org/10.21012/FC11.0923105

CARBONATION AND CHLORIDE-INDUCED CORROSION FATIGUE LIFE PREDICTION OF REINFORCED CONCRETE

RAM LAL RIYAR[*1], **SONALI BHOWMIK**[*2]

[*]Department of Civil Engineering
National Institute of Technology Rourkela, Odisha, India
e-mail[1]: 521ce1013@nitrkl.ac.in
e-mail[2]: bhowmiksonali@nitrkl.ac.in

Key words: Corrosion, Reinforced Concrete, Fatigue Life, Carbonation

Abstract. Reinforcement corrosion has been identified as the leading cause of reinforced concrete structural degradation. Concrete structures are more susceptible to environmental factors such as corrosion, which affects the component's service life. As concrete is a heterogeneous material, it is difficult to understand the fatigue crack growth phenomenon in the combined effect of carbonation and chloride-induced corrosion. Corrosion accelerates the crack growth rate, and the combined action of corrosion and fatigue ultimately reduces the concrete structure's strength, durability, and fatigue life. Corrosion fatigue life assessment is essential for the design of reinforced concrete structures. An important challenge in predicting the corrosion-fatigue life is investigating the effect of corrosion due to carbonation and chloride ingress with fatigue crack propagation. A probabilistic fatigue life prediction model based on Fick's law of diffusion has developed by incorporating important parameters of carbonation-induced corrosion, chloride ingress corrosion, and environmental aggressiveness with time. Chloride and carbon dioxide ingress, corrosion pit growth, stress intensity factor, frequency of the cyclic load, humidity, temperature, and combined chloride and carbon dioxide attacks are considered.

1 INTRODUCTION

Corrosion is a prevalent phenomenon seen in several categories of civil infrastructure. The long-term durability of reinforced concrete (RC) structures is significantly compromised by the corrosive effects of chloride-induced and carbonation-induced corrosion. In addition, the permeation of chloride in concrete structures is influenced by several environmental factors, including temperature and relative humidity. The diffusivity of carbon dioxide and chloride has a substantial influence on the corrosion process in concrete structures. In RC structures, material degradation will be brought on by both repeated loads and environmental factors. The main causes of RC structure performance degradation are fatigue damage and reinforcement corrosion. Corrosion-damaged RC structures have a more complicated fatigue failure process than RC structures without corrosion. The explanation is that the collapse of RC structures brought on by the combined action of corrosion and fatigue is a linked process of their reciprocal effect rather than a simple superposition of these two failure elements.

Concrete carbonation is a chemical reaction that occurs between penetrated carbon dioxide and calcium hydroxide (a result of alkaline cement hydration). This reaction lowers the alkalinity of the concrete, destroying the passive layer that has developed around the steel bars. This process leads to initiate steel corro-

sion [1, 2]. Carbonation, in general, does not influence the qualities of the concrete material itself and even improves internal pore structures and enhances density through the formation of carbonation salts. When the carbonation is near the surface of the reinforcement material embedded in the concrete, the pore solution with a low pH value might make the passivation coating on its surface unstable, ultimately dissolving it and causing reinforcement material corrosion. In contrast to chloride-induced steel corrosion, concrete carbonation results in homogenous deterioration of the reinforcing surface [3]. Generally, reinforced concrete often experiences the simultaneous influence of many corrosion causes rather than being affected by a single one alone. These elements tend to mutually reinforce one another, resulting in heightened and more severe deterioration of the reinforced concrete. One potential effect of carbonation on concrete is the elevation of free chloride ion levels. This is due to the reaction between carbon dioxide and Friedel's salt, which leads to the conversion of bound chlorides into free chlorides [4, 5].

The degradation of structural performance in RC structures is considerably exacerbated by the reinforcement corrosion and fatigue damage brought on by different repetitive loadings. Additionally, the stress concentration caused by the rebar's pitting corrosion damage will lead to the early initiation of a fatigue fracture [6, 7]. The structural performance decay caused by fatigue damage at the pit-induced stress concentration will thereafter worsen significantly, which will ultimately result in a significant decrease in the dependability and serviceability of deteriorating RC structures [8, 9]. As a result, coupled corrosion-fatigue damage becomes more harmful to RC structures that are already failing, necessitating an urgent need for service life evaluation. Corrosion when coupled with fatigue on the structure leads to rapid degradation of the strength, loss of cross section of rebars and increased crack propagation rate compared to structure only under fatigue loading. Efforts have been made to learn how the serviceability of the structures have been affected. This paper mainly deals with the crack propagation in the structure under fatigue loading coupled with the corrosion effect. The chloride ion transport equation in concrete is formulated considering multiple factors such as carbonization, load, saturation, relative humidity, and temperature. The following model considers the corrosion pit as a notch, a concept that many researchers have used to find the fatigue life of the structure coupled with corrosion in probabilistic approaches.

2 CORROSION MECHANISM IN REINFORCED CONCRETE

Concrete has an alkaline character, as seen by its pore solution pH range of 12-13, which effectively passivates the embedded reinforcing bars. The passivation process of steel is compromised by the presence of chloride ions or a decrease in the alkalinity of concrete resulting from carbonation. The carbonation process in concrete involves the chemical interaction between portlandite $(Ca(OH)_2)$ present in the cement matrix and carbon dioxide (CO_2) gas, resulting in the formation of calcite $(CaCO_3)$. The process of carbonation occurs due to the chemical reaction between carbon dioxide and calcium hydroxide present in concrete. The process involves the dissolution of carbon dioxide gas in water, resulting in the formation of carbonic acid (H_2CO_3). This acid then combines with calcium hydroxide, leading to the precipitation of calcium carbonate $(CaCO_3)$. The calcium carbonate mostly accumulates and forms a lining inside the pores. The reduction in hydroxyl ions (OH^{-1}) results in a decrease in the pH of the pore water, transitioning from a value over 12.5 to below 9.0. This shift in pH destabilises the passive layer, which may lead to the onset of general corrosion under the condition that there is a enough presence of oxygen and water in the vicinity of the rebar.

Chloride-induced corrosion is often more hazardous and costly to remediate, but carbonation-induced corrosion of reinforcement bars may impact a broader array of re-

inforced concrete structures on a bigger magnitude. Both corrosion methods may lead to a substantial decrease in the structural load-bearing capacity by diminishing the cross-sectional area of the steel reinforcement bars, impairing the steel's ability to elongate, and inducing extensive cracking in the concrete. The formation of a compact oxide coating on the surface of reinforcing elements may effectively inhibit corrosion, since high alkalinity cement hydration products are present inside the concrete. The depassivation property of chloride ions is responsible for the corrosion of reinforcement material in concrete. When a sufficient amount of chloride ions permeate the oxide film via interconnected pores and cracks, the pH of the surrounding pore solution decreases, leading to the destruction of the protective film. Consequently, corrosion of the reinforcement material is initiated. Moreover, it is of utmost significance to note that the chloride ions possess the ability to function as catalysts, so facilitating the corrosion process without undergoing any consumption themselves [10]. Hence, the ingress of chloride ions into the concrete matrix perpetuates the degradation of the concrete structure, so exemplifying the fundamental attribute of chloride corrosion. Furthermore, in contrast to the homogeneous corrosion resulting from concrete carbonation, chloride-induced steel corrosion manifests as pitting corrosion [11].

3 CORROSION-FATIGUE MODEL

In light of the above succinct description, it is important to appropriately address the link between crack formation and corrosion propagation in the fatigue life prediction of RC bridges. This study consider corrosion pit as a notch in fatigue life evaluation models for RC bridges. Considerations include chloride intrusion, corrosion pit development, severe concrete cracking, fatigue crack growth, and effect of enviromental factors on corrosion. This section introduces an approach for predicting the corrosion-fatigue life of RC bridges. Three steps make up the full process: (1) development of fatigue cracks prior to the start of corrosion; (2) competition between the growth of corrosion pits and fatigue cracks; and (3) identification of structural collapse. This framework accounts for cyclic load, corrosion pit-induced stress concentration, concrete cracking, seasonal environmental change, and carbonation effect on chloride ion ingress.

Corrosion of the reinforcement is mostly brought on by chloride intrusion. Chloride infiltration causes reinforcement to get depassivated, which then triggers the beginning of steel bar corrosion. The process of chloride ions entering concrete is complicated and involves a number of different transport mechanism. The process of diffusion is thought to be the main mechanism of chloride ion infiltration into concrete. The diffusion procedure is explained by Fick's second law.

$$\frac{\partial C(x,t)}{\partial t} = D_{cl}.\frac{\partial^2 C(x,t)}{\partial x^2} \tag{1}$$

Where D_{cl} is the chloride diffusion coefficient $(cm^2/year)$, $C(x,t)$ is the chloride ion concentration (percentage weight of concrete), t is the time (after concrete exposed to chloride source), x is the depth in concrete in the diffusion direction. Solution for this differential equation is given by:

$$C_{(x,t)} = C_0[1 - erf\frac{x}{2\sqrt{D_c t}}] \tag{2}$$

Where, C_0 is the equilibrium chloride concentration on the concrete surface, and erf is the Gaussian error function.

The penetration of chloride ions leads to the depassivation of the reinforcing material, which in turn triggers the onset of corrosion in the rebars. The time at which corrosion begins is mostly influenced by the concentration of chloride ions, the properties of the concrete, chloride diffusion coefficient and the thickness of the concrete cover. The corrosion initiation time is determined by the conditions that $C(x,t)$ approaches threshold chloride concentration (C_{th}) and the depth x equals the concrete cover thickness.

$$T_i = \frac{C_0^2}{4D_{cl}}[erf^{-1}(1 - \frac{C_{th}}{C_s})] \tag{3}$$

Where, T_i is the corrosion initiation time (year), C_0 is the concrete cover thickness (cm), C_{th} is the threshold chloride concentration which is the value at which the passivation layer of reinforcement is destroyed, (percentage weight of concrete), and C_s is the surface chloride concentration (percentage weight of concrete). A number of surface chloride concentration values are considered so that for different C_s values, the crack length can be calculated. Value of C_s changes depending upon the position of the structure from sea shore, atmospheric conditions and seasonal changes etc. C_s according to seasonal changes is taken into consideration for pointing out the real-life scenario for calculating the crack length at different situations. A range has been taken to find the C_s in different seasons shown in Table 1.

Table 1: Range of surface chloride concentration in different seasons

Season	C_s range(% wt of concrete)
Winter	0.15-0.4
Spring	0.4-0.58
Summer	0.5-0.87
Autmn	0.3-0.68

The diffusion rate of chloride in unsaturated concrete has been shown to be significantly influenced by several characteristics, including porosity, environmental elements such as temperature and relative humidity, and service circumstances such as load case and stress state. The estimation of the diffusion coefficient D_{cl} for unsaturated concrete under loading and carbonation conditions may be conducted using the multifactor technique in the following manner:

$$D_{cl} = D_{ref}.f_1(t).f_2(T).f_3(RH).f_4(d).f_5(C).f_6(R) \quad (4)$$

where D_{ref} is the diffusion coefficient reference chloride ion concentration. The functions $f_1(t)$, $f_2(T)$, $f_3(RH)$, $f_4(d)$, $f_5(C)$, $f_6(R)$ are responsible for explaining the relationship between chloride diffusion coefficient and many factors such as concrete age, temperature, internal relative humidity, concrete degradation, electrostatic interaction, and chloride binding capacity due to carbonation. Based on the compound sphere model, Xi and Bazant [12] suggested a model for forecasting the effective diffusion coefficient of cement-based composites, which is written as:

$$D_{ref} = D_p \frac{2(1 - V_a)}{2 + V_a} \quad (5)$$

Where, V_a, and D_p are aggregate volume fraction, aggregate diffusion coefficient and diffusion coefficient of hardened cement paste respectively. The chloride diffusion coefficient of cement paste was established based on an extensive collection of experimental data as: [2]

$$D_p = \frac{2.14 \times 10^{-10} \phi_0^{2.75}}{\phi_0^{2.75}(3 - \phi_0) + 14.44(1 - \phi_0^{2.75})} \quad (6)$$

The porosity of cement paste, denoted as ϕ_0, may be defined by the water-cement ratio (w/c) and the rate of cement hydration (h) [45].

$$\phi_0 = \frac{w/c - 0.17h}{w/c + 0.32} \quad (7)$$

In order to make the computation simpler, h can also be computed using the following formula, which was discovered by regression analysis using the experimental data from published literature [14]:

$$h = 0.716 t_1^{0.0901} exp(\frac{-0.103 t_1^{0.0719}}{w/c}) \quad (8)$$

where t_1 is curing time in days.

The phenomenon of cement hydration is well acknowledged to result in a progressive reduction in porosity and a subsequent limitation of chloride diffusion over time. The impact of concrete age on the chloride diffusion coefficient in concrete may be expressed as:

$$f_1(t) = (\frac{t_{ref}}{t})^m \quad (9)$$

The reference age, denoted as t_{ref}, is typically set to 28 days. The decay index of time is represented by the variable m=0.15.

The diffusion coefficient of chloride in concrete is influenced by temperature due to its impact on the absorption heat and the frequency of thermal vibration of the diffusant. The relationship between temperature and chloride diffusion coefficient in concrete may be described by Arrhenius' law [16].

$$f_2(T) = exp[\frac{U_T}{r}(\frac{1}{T_{ref}} - \frac{1}{T})] \quad (10)$$

The activation energy of the diffusion process (U_T) may be expressed in kilojoules per mole (kJ/mol). In this case, U_T is equal to 41800 J/mol. T_0 represents the reference temperature, which is 273.15 K. T denotes the current temperature in Kelvin (K).

Furthermore, the chloride diffusion coefficient in concrete is humidity dependant. The effect of internal relative humidity on the chloride diffusion coefficient in concrete is shown by [15] as Eq. 11.

$$f_3(RH) = [1 + \frac{(1 - RH^4)}{(1 - RH_c^4)}]^{-1} \quad (11)$$

The critical humidity, denoted as RH_c, is the point at which the diffusion coefficient decreases by 50% between its highest and lowest values. Specifically, RH_c is equal to 75%. The presence of external elements such as temperature, shrinkage, and creep may result in the development of early faults inside the material. Microscopic cracks might potentially develop throughout the course of maintaining and using concrete structures over an extended period of time. The acceleration of chlorine transport in concrete is attributed to the presence of micro fractures, therefore necessitating the consideration of the impact of early flaws on chloride transport in concrete. The phenomenon of concrete cracking is intricately linked to the water-to-cement ratio (w/c) of concrete, denoted as Eq. 12.

$$f_4(d) = \frac{1}{3}[1000(\frac{w}{c})^2 - 1050(\frac{w}{c}) + 287] \quad (12)$$

The movement of chloride ions is impeded by the electrostatic field generated by the presence of other ions in the solution. This effect may be quantified as stated in reference [17].

$$f_5(c) = 1 - k_{ion}.C^{\gamma'} \quad (13)$$

where k_{ion} and γ' are two constants, k_{ion} = 8.333 and γ' = 0.5.

Certain chloride ions undergo reactions with hydration products, resulting in the formation of Friedel's salt. Additionally, a portion of these ions are adsorbed onto the surface of hydrated calcium silicate or enclosed inside the layers of C-S-H during the transportation process [18]. The chloride binding capacity plays a significant role in determining the chloride diffusion coefficient in concrete, as shown by previous research [19]. Given the impact of concrete carbonation on the binding capacity of chloride ions expressed as Eq. 14.

$$f_6(R) = \frac{1}{(1 + \xi R)} \quad (14)$$

where ξ is the reduction coefficient of chloride binding capacity caused by carbonation and R represents the value that evaluates the chloride binding capacity of concrete shown in Eq.15.

$$R = \begin{cases} \frac{\alpha}{(1+\beta C_{cl})^2} & C_{cl} \leq 1.77 kg/m^3 \\ \alpha' \beta' C_{cl}^{\beta'-1} & C_{cl} \leq 1.77 kg/m^3 \end{cases} \quad (15)$$

The process of carbonation in concrete has dual effects on the movement of chloride ions. One aspect to consider is that carbonation leads to an expansion of the solid phase inside concrete, which may be related to the interaction between the internal alkaline components of the concrete and CO_2. This expansion results in a reduction of porosity and hinders the passage of chloride ions. In contrast, the process of carbonation has an impact on the diffusion of chloride ions inside concrete by altering the mechanism of chloride binding. The process of carbonation has the potential to disrupt the adsorption and binding mechanisms, resulting in the eventual release of chlorides that were previously bound, into the pore solution. Consequently, the process of carbonation leads to an elevation in the concentration of free chlorides within the pore

solution, thus expediting the diffusion of chlorides.

The pitting depth in specimen is given by an integration of equation proposed by [20] for total maximum pit depth in terms of time and corrosion rate measured as current density ($\mu A/cm^2$).

$$P(t) = 0.011R_0 \int i_{corr}(t)dt \tag{16}$$

Where, p(t) is the corrosion pit depth (mm), R_0 is the ratio of the maximum pit depth to uniform corrosion depth, $i_{corr}(t)$ is the corrosion current density. Corrosion current density $i_{corr}(t)$ is given by [21] proposed at any time t as a function of concrete water/cement ratio (w/c) and the cover and is given by

$$i_{corr}(t) = 32.1(1 - \frac{w}{c})^{-1.64}.(t - T_1)^{-0.29}/C_0 \tag{17}$$

Where, $\frac{w}{c}$ is the water/cement ratio and can be estimated from the Bolomey's formula as $w/c = \frac{27}{f_c+13.5}$ is the compressive strength of concrete (MPa), C_0 is the concrete cover thickness (mm).

After substituting the values of $i_{corr}(t)$ in Eq.16, updated corrosion pit depth is :

$$p(t) = A(t - T_i)^{0.71} \tag{18}$$

where $A = \frac{0.0116*R_0*32.1*(1-w/c)^{-1.64})}{0.71C_0}$.

As corrosion progresses and when the crack width reaches a certain threshold crack width, rate of crack propagation increases. [22] considered this rapid progression and proposed an additional factor called acceleration coefficient, which gives the accelerated crack length after certain time period from corrosion initiation. The modified equation for corrosion pit depth is:

$$P(t) = 0.011R_0 \int_{T_i}^{t} i_{corr}(t)dt \tag{19}$$

There were two models proposed by [23] for finding out the rate of change of pitting depth with respect to time caused by pitting corrosion. First one considered the pitting depth as a notch in the beam. And the other model considered the pitting depth as a surface crack. The present working model considered the pitting depth as a notch. The fatigue crack length of concrete is given by:

$$\frac{da}{dt} = C(\triangle K)^m f \tag{20}$$

Where, $\frac{da}{dt}$ is the fatigue crack growth rate (mm/sec), C, m are the fitting parameters estimated from experimental data, f is the frequency of cycles, $\triangle K$ is the stress intensity factor range $(MPa\sqrt{m})$ and can be calculated as

$$\triangle K = Y \triangle \sigma \sqrt{\pi a} \tag{21}$$

Where, Y is the geometric correction factor, $\triangle \sigma$ is the stress range of tensile rebar (MPa), a is the fatigue crack length. When taking pitting corrosion into account, the equation is adjusted to account for the depth of pitting. The amended equation is as follows:

$$\frac{da}{dt} = C(\triangle K_{p(t)})^m f \tag{22}$$

Where, $\triangle K_{p(t)}$ is the stress intensity factor range at the root of corrosion pit. This stress intensity factor was determined by [24] which is given by:

$$\triangle K_{p(t)} = Y \triangle \sigma \sqrt{\pi(a + p(t)[1 - e^{-\frac{a}{p(t)}(k_t^2-1)}} \tag{23}$$

Where 'a' is the equivalent initial flaw size(mm) is given by:

$$a = \frac{1}{A}(\frac{\triangle K_{th}}{\triangle \sigma_f Y})^2 \tag{24}$$

Where, $\triangle K_{th}$ is the threshold stress intensity factor range $(MPa\sqrt{m})$ and k_t is the stress concentration factor and is given by:

$$k_t = 3.453(p(t) + 0.0056)^{0.239} \tag{25}$$

Y is a geometric function and is determined using Eq.26.

$$Y = G(0.752 + 1.286\beta + 0.37H^3) \tag{26}$$

Where, $G = 0.92\left(\frac{2}{\pi}\right)Sec\beta\sqrt{\frac{tan\beta}{\beta}}$, $H = 1 - Sin\beta$, $\beta = \frac{\pi d}{2D}$, d is corrosion pit depth P(t), D is the diameter of the rebar. By substituting Eq.23 in Eq. 22 and $f = \frac{dN}{dt}$, the following expression for rate of crack propagation (mm/cycle) is obtained.

$$\frac{da'}{dN} = C[Y\triangle\sigma\sqrt{\pi(a + p(t)[1 - e^{-\frac{a}{p(t)}(k_t^2-1)}]}]^m \quad (27)$$

Where, $(a+p(t)[1-e^{-\frac{a}{p(t)}(k_t^2-1)}])$ is called as effective crack length and is denoted by a'. This pit depth expression is used for a' and used to find the rate of crack propagation per cycle. The Eq. 27 rewritten as:

$$\frac{da^{'}}{C[Y\triangle\sigma\sqrt{\pi a^{'}}]} = dN \quad (28)$$

The integration process yields the number of cycles necessary for creating an effective fracture length, denoted as a'. The resulting equation is observed as Eq.29.

$$N = \frac{a^{1-\frac{m}{2}} - (a')^{1-\frac{m}{2}}}{\left(\frac{m}{2} - 1\right) * C * Y^m * \sigma^m \pi^{m/2}} \quad (29)$$

Where, a is the equivalent initial flaw size, a' is the effective crack length, m and c are material Paris law constants, Y is the geometric correction factor, σ is the stress applied.

4 RESULT AND DISCUSSION

The combined effect of concrete carbonation and repetitive stress significantly impacts the structural integrity of reinforced concrete structures and diminishes their operational lifespan. In this study, a model is developed to estimate the corrosion-fatigue life of reinforced concrete subjected to both carbonation and repetitive loading considering other environmental factor affecting it such as concrete age, temperature, internal relative humidity, concrete degradation, electrostatic interaction, and chloride binding capacity due to carbonation. The observations are calculated till the 40 years of age of structure. Material properties and other parameter values used for calculation of different variables are tabulated in Table 2.

Table 2: Depicting the values for different parameters

Material Properties	Value
Elastic modulus of concrete	31,500 MPa
Elastic modulus of rebar	210 GPa
Yield strength of rebar	480 MPa
Threshold stress intensity factor range	3.157 $(MPa\sqrt{m})$
Concrete poisson ratio	0.2
Diameter of uncorroded rebar	25 mm
Concrete cover thickness	35 mm
Threshold chloride concentration	0.045 MPa
Chloride diffusion coefficient	0.4 cm2 /year
Water to cement ratio of concrete	0.4
Porous zone of concrete around rebar	0.002 mm
Creep coefficient of concrete	2
Maximum to uniform pit depth ratio	4

The findings indicate that the primary factor contributing to the overall fracture length is the depth of corrosion pits. The overall equivalent fracture length and pit depth exhibit variations for varying surface chloride concentrations.

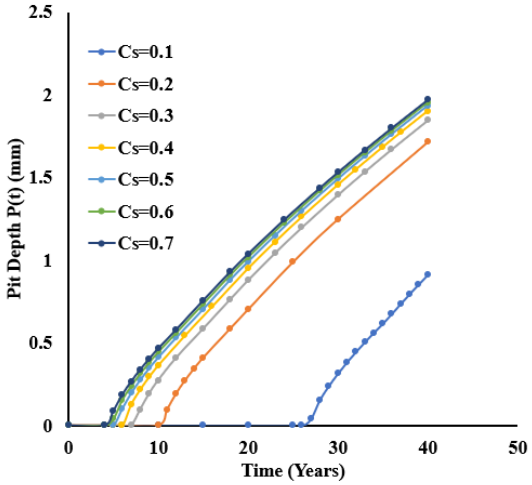

Figure 1: Variation of Corrosion Pit depth with time (years) with different surface ion concentration without considering environmental and carbonation effect.

Figure 1 demonstrate the corrosion pit depth fluctuation over time (years) with varying surface ion concentration without taking ambient

and carbonation effect into account. The corrosion initiation time for C_s= 0.1, 0.2, 0.3, 0.4, 0.5, 0.6, 0.7 is calculated as 26.82,10.39, 7.38, 6.08, 5.32, 4.83 4.47, 4.2 years respectively. Whereas, Figure 2 shows the environmental and carbonation effects on corrosion pit depth over time (years) with varying surface ion concentrations. The combined cabonation and chloride ingress corrosion decrease the corrosion initiation time. The rise in chloride content is accompanied by an increase in both pit depth and crck length.

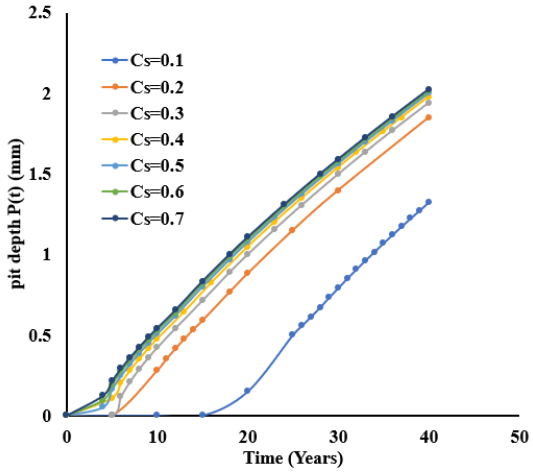

Figure 2: Environmental and carbonation effects on corrosion pit depth over time (years) with varying surface ion concentrations.

During a certain three-month period, which may be considered a season, the propagation of crack development is seen to align with a curve that corresponds to the concentration of chloride on the surface. For instance, throughout the summer season spanning three months, the fracture propagation curve aligns with an average surface chloride concentration of around 0.6. The plot of crack growth rate (da/dN) variation with time and with surface ion concentration ignoring environmental and carbonation effects is shown in Figure 3, and with considering environmental factors and carbonation effects in Figure 4. The crack propagation rate increases when carbonation and chloride penetration are coupled with environmental effect. The time at which first crack starts also decreases when carbonation and chloride penetration are coupled.

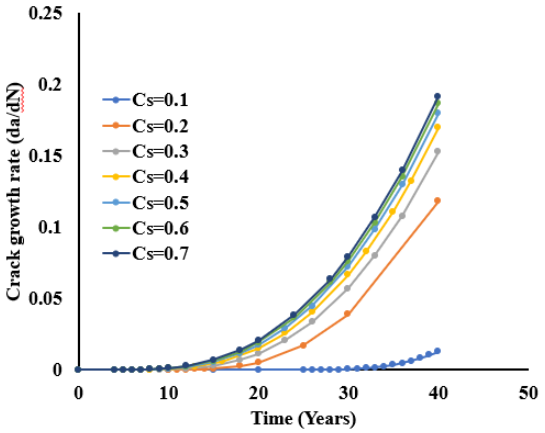

Figure 3: Crack growth rate (da/dN) variation with time and with surface ion concentration ignoring environmental and carbonation effects.

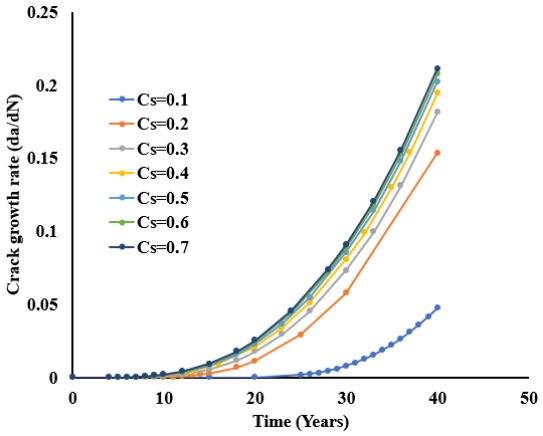

Figure 4: Environmental and carbonation effects on Variation of the crack growth rate (da/dN) with time and surface ion concentration.

When carbonation and chloride penetration corrosion occur simultaneously with the effects of fatigue loading, crack growth rate and crack length is also observed to be increased. From the Figure 5, It can be seen that crack growth rate without considering the environmental and carbonation effect in coupled corrosion fatigue model is less than that observed with consideration the evvironmental factors and carbonation at 40 years. The results of the predictions fluctuate depending on whether the seasonal fluctuation is taken into account, particularly when

the environment is quite hostile. As a result, it is advised that the influence of seasonal fluctuation should be taken into account for corrosion fatigue modelling.

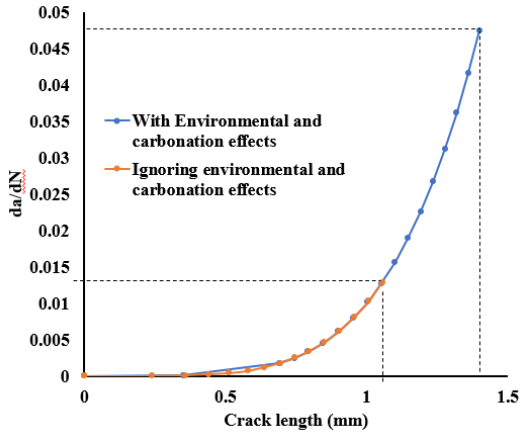

Figure 5: Relationship between the crack development rate (da/dN) and crack length for a C_s value of 0.1.

5 CONCLUSIONS

Based on Fick's second law, considering carbonation, load, saturation, humidity, temperature and other factors, the crack growth rate model under coupled corrosion fatigue in concrete is established. The combined effects of corrosion and fatigue have a considerable impact on the degradation of structures, leading to a substantial decrease in their remaining service life. The presence of corrosion pits leads to localised stress concentration, which in turn promotes the initiation and growth of fatigue cracks. Neglecting the influence of carbonation and seasonal environmental effect may lead to an overestimation of the fatigue life of structures. Hence, damage analysis for the seasonal climate and associated concrete and rebar requires further research. Additionally, because of how challenging natural environmental conditions are for the beginning and spread of corrosion and fatigue cracks, considerable theoretical and experimental research is also necessary, including modelling of geographic variability and variable load.

REFERENCES

[1] J. Liu, Q. Qiu, X. Chen, X. Wang, F. Xing, N. Han, Y. He 2016. *Degradation of fly ash concrete under the coupled effect of carbonation and chloride aerosol ingress,Corrosion*, (112, 2016, pp.364-372).

[2] Q. Zhang 2016. *Mathematical modeling and numerical study of carbonation in porous concrete materials,Corrosion*, (281, 2016, pp.19-27).

[3] M.F. Bertos, S.J.R. Simons, C.D. Hills, P.J. Carey 2004. *A review of accelerated carbonation technology in the treatment of cement-based materials and sequestration of CO2,Journal of Hazardous Materials*, (112 (3), 2004, pp.193-205).

[4] A.K. Suryavanshi, R.N. Swamy 1996. *Stability of Friedel's salt in carbonated concrete structural elements,Cement and Concrete Research*, (26 (5), 1996, pp.729-741).

[5] J. Liu, Q. Qiu, X. Chen, F. Xing, N. Han, Y. He, Y. May 2017. *Understanding the interacted mechanism between carbonation and chloride aerosol attack in ordinary Portland cement concrete, Cement and Concrete Research*, (95, 2017, pp.217–225).

[6] Xu S, Wang Y 2015. *Estimating the effects of corrosion pits on the fatigue life of steel plate based on the 3D profile. Int J Fatigue*, (72, 2015, pp.27-41).

[7] Yang D, Yi T, Li H 2017. *Coupled fatigue-corrosion failure analysis and performance assessment of RC bridge deck slabs. J Bridge Eng*, (22 (10), 2017, pp.1-9).

[8] Larrosa NO, Akid R, Ainsworth RA 2018. *A review of damage tolerance models. Taylor & Francis*, (63 (5), 2018, pp.283–308).

[9] Ma Y, Guo Z, Wang L, Zhang 2020. *Probabilistic life prediction for reinforced concrete structures subjected to seasonal corrosion-fatigue damage. J Struct Eng*, (146 (7), 2015, pp.1–17).

[10] C.A. Apostolopoulos, S. Demis, V.G. Papadakis 2013. *Chloride-induced corrosion of steel reinforcement–Mechanical performance and pit depth analysis, Construction and Building Materials*, (38, 2013, pp.139–146).

[11] A. Neville 1995. *Chloride attack of reinforced concrete: an overview, Materials and Structures*, (28 (2), 1995, pp.63–70).

[12] Xi, Y. & Bazant, Z. P 1999. *Modeling chloride penetration in saturated concrete, Journal of Materials in Civil Engineering*, (11 (1), 1999, pp.58-65).

[13] Zheng J, Zhou X 2008. *Analytical solution for the chloride diffusivity of hardened cement paste. J Mater Civ Eng*, (20 (5), 2008, pp.384-391).

[14] Hansen TC 1986. *Physical structure of hardened cement paste. A classical approach, Materials and Structures*, (19 (6), 1986, pp.423–436).

[15] da Costa A, Fenaux M, Fern´ andez J, Sanchez ´ E, Moragues A 2013. *Modelling of chloride penetration into non-saturated concrete: Case study application for real marine offshore structures, Constr Building Material*, (43 (6), 2013, pp.217-224).

[16] Xi YP, Bazant ZP 1999. *Degree of hydration and gel/space ratio of high-volume fly ash/cement systems. Cement Concrete Research*, (11(1), 1999, pp.58–65).

[17] Ababneh A, Benboudjema F, Xi YP 2003. *Chloride penetration in nonsaturated concrete, J Mater Civ Eng*, (15(2), 2003, pp.183-191).

[18] Yuan Q, Shi CJ, De Schutter G, Audenaert K, Deng DH 2009. *Chloride binding of cement based materials subjected to external chloride environment, Constr Build Mater*, (23(1), 2009, pp.1-13)

[19] Luping T, Nilsson LO 1993. *Chloride binding capacity and binding isotherms of OPC pastes and mortars. Cem Concr Res*, (23(2), 1993, pp.247-253).

[20] Vu, Kim and Stewart, Mark G and Mullard, John 2005. *Corrosion-induced cracking: experimental data and predictive models, ACI structural journal*, (102 (5), 2005, pp.719)

[21] Vu, Kim Anh T and Stewart, Mark G 2000. *Structural reliability of concrete bridges including improved chloride-induced corrosion models, Structural safety*, (22 (4), 2000, pp.313-333)

[22] Ma, Y., Wang, L., Zhang, J., Xiang, Y., Peng, T., & Liu, Y. 2015 *Hybrid uncertainty quantification for probabilistic corrosion damage prediction for aging RC bridges, Journal of Materials in Civil Engineering*, (27 (4), 2015, pp.141-152)

[23] Guo, Zhongzhao and Ma, Yafei and Wang, Lei and Zhang, Jianren 2015 *Modelling guidelines for corrosion-fatigue life prediction of concrete bridges: Considering corrosion pit as a notch or crack, Engineering Failure Analysis*, (105, 2019, pp.883-895)

[24] Liu, Yongming and Mahadevan, Sankaran 2015 *Fatigue limit prediction of notched components using short crack growth theory and an asymptotic interpolation method, Engineering Fracture Mechanics*, (76 (15), 2009, pp.2317-2331)